Cellular Encapsulation Enhances Cardiac Repair

Rebecca D. Levit, Natalia Landázuri, Edward A. Phelps, Milton E. Brown, Andrés J. García, Michael E. Davis, Giji Joseph, Robert Long, Susan A. Safley, Jonathan D. Suever, Alicia N. Lyle, Collin J. Weber and W. Robert Taylor

The online version of this article, along with updated information and services, is located on the World Wide Web at:
http://jaha.ahajournals.org/content/2/5/e000367

Cellular Encapsulation Enhances Cardiac Repair

Rebecca D. Levit, MD;* Natalia Landázuri, PhD;* Edward A. Phelps, PhD; Milton E. Brown, BS; Andrés J. García, PhD; Michael E. Davis, PhD; Giji Joseph, MS; Robert Long, Jr, PhD; Susan A. Safley, PhD; Jonathan D. Suever, PhD; Alicia N. Lyle, PhD; Collin J. Weber, MD; W. Robert Taylor, MD, PhD

Background—Stem cells for cardiac repair have shown promise in preclinical trials, but lower than expected retention, viability, and efficacy. Encapsulation is one potential strategy to increase viable cell retention while facilitating paracrine effects.

Methods and Results—Human mesenchymal stem cells (hMSC) were encapsulated in alginate and attached to the heart with a hydrogel patch in a rat myocardial infarction (MI) model. Cells were tracked using bioluminescence (BLI) and cardiac function measured by transthoracic echocardiography (TTE) and cardiac magnetic resonance imaging (CMR). Microvasculature was quantified using von Willebrand factor staining and scar measured by Masson's Trichrome. Post-MI ejection fraction by CMR was greatly improved in encapsulated hMSC-treated animals (MI: 34±3%, MI+Gel: 35±3%, MI+Gel+hMSC: 39±2%, MI+Gel+encapsulated hMSC: 56±1%; n=4 per group; $P<0.01$). Data represent mean±SEM. By TTE, encapsulated hMSC-treated animals had improved fractional shortening. Longitudinal BLI showed greatest hMSC retention when the cells were encapsulated ($P<0.05$). Scar size at 28 days was significantly reduced in encapsulated hMSC-treated animals (MI: 12±1%, n=8; MI+Gel: 14±2%, n=7; MI+Gel+hMSC: 14±1%, n=7; MI+Gel+encapsulated hMSC: 7±1%, n=6; $P<0.05$). There was a large increase in microvascular density in the peri-infarct area (MI: 121±10, n=7; MI+Gel: 153±26, n=5; MI+Gel+hMSC: 198±18, n=7; MI+Gel+encapsulated hMSC: 828±56 vessels/mm^2, n=6; $P<0.01$).

Conclusions—Alginate encapsulation improved retention of hMSCs and facilitated paracrine effects such as increased peri-infarct microvasculature and decreased scar. Encapsulation of MSCs improved cardiac function post-MI and represents a new, translatable strategy for optimization of regenerative therapies for cardiovascular diseases. (*J Am Heart Assoc.* 2013;2:e000367 doi: 10.1161/JAHA.113.000367)

Key Words: angiogenesis • cardiovascular diseases • heart failure • ischemia • myocardial infarction

Cell-based therapies have great potential to decrease the morbidity and mortality of cardiovascular diseases (CVDs) due to their ability to augment endogenous repair or to regenerate damaged tissues. After myocardial infarction (MI), the endogenous regenerative capacity of the human heart is unable to replace the damaged tissue and a fibrotic, noncontractile scar forms. Initially, stem cells were thought to exclusively differentiate or transdifferentiate into mature cells such as cardiomyocytes and endothelial cells and subsequently incorporate into existing tissues.[1,2] Although this has been shown to happen in some instances, the dominant effect of most stem cells likely occurs through paracrine mechanisms.[3–6] These paracrine mechanisms are thought to be particularly relevant to adult bone marrow-derived stem cells, such as mesenchymal stem cells (MSCs), which promote angiogenesis,[7] prevent apoptosis,[8] modulate immune response,[9] recruit stem and progenitor cells,[10] and facilitate beneficial remodeling.[11] A major barrier to the success of stem cells is poor retention and survival of transplanted cells in the heart, which can be >10% as early as 1 hour after injection in most human[12–16] and large animal studies.[17,18] Transplanted cells can be mechanically ejected from the heart by myocardial contraction, transported away in lymphatic or vascular channels, migrate from the site of injection, or they

may simply die.[19,20] Thus, strategies focused on increasing cell retention and viability have great potential to enhance the therapeutic effects of cell-based therapies.

MSCs are a promising cell type for stem cell therapy for CVDs. Autologous hMSCs can be obtained from adult bone marrow, adipose tissue, as well as other tissues, and are relatively easy to culture and expand ex vivo. They possess the ability to differentiate into endothelial cells and cardio-myocytes, but likely have a greater effect through paracrine mechanisms.[4] hMSCs are highly secretory, producing a variety of immune modulatory, proangiogenic, and antiapop-totic growth factors and cytokines that act in a paracrine manner to preserve tissue integrity and function after ischemia.[4,7–9] In response to ischemia, hMSCs up-regulate secretion of cytokines including vascular endothelial growth factor (VEGF), fibroblast growth factor (FGF), placental growth factor (PlGF), and have been shown to facilitate tissue preservation in small[7] and large animal studies.[21,22] Results from early phase I clinical trials suggest that autologous hMSC administered using a catheter-based approach is a feasible and safe approach that may have a modest effect on cardiac function in ischemic cardiomyopathy.[23,24]

Cell encapsulation represents a novel and translatable strategy to augment transplanted cell survival and retention in a variety of target tissues including the heart.[25–27] Capsules function as a mechanical barrier preventing washout of transplanted cells and may partially insulate cells from components of the immune system such as inflammatory cells and immunoglobulins.[28] The functional porosity of alginate allows proteins and small molecules access to encapsulated cells and permits secretion of stem cell-produced growth factors and cytokines into the surrounding tissue. Encapsula-tion of porcine islets is currently in clinical trials as treatment for type I diabetes.[29] As proof of principle, we previously demonstrated that encapsulated hMSCs augment neovascu-larization in a murine model of hind limb ischemia and produce a wide array of proangiogenic cytokines.[28]

To translate this strategy into a small animal MI model, we used a composite biomaterials approach. Alginate-encapsu-lated hMSCs were implanted in a biocompatible poly-(ethylene glycol) (PEG) hydrogel patch to secure the encapsulated cells to the injured heart.[30] Other hydrogels including alginate have been designed to deliver cells or growth factors and are in clinical and preclinical trials.[31–33] In a large animal model or in humans, capsules may also be amenable to direct intramyocardial injection or intracoronary catheter delivery. Capsule size relative to the rodent heart lends itself to the use of the hydrogel patch. The hydrogel patch used in this study has an open network structure and low protein retention, permitting free diffusion of cytokines and small molecules.[30,33] Importantly the gelation time can be manipulated as it is applied to the myocardium, localizing the patch to the site of myocardial infarction.

The need to use stem cell therapies for CVD is clear: preserving left ventricular function would reduce the morbidity and mortality associated with MI, a leading cause of death in the United States.[34] Many clinical trials with various adult-derived stem cells have likely been limited by poor cell survival and retention.[12–16,24,35–37] In this study we present a novel encapsulated cell patch made up of encapsulated hMSC attached to the damaged heart by a PEG hydrogel. This patch allows sustained stem cell presence at the site of injury and prolonged paracrine factor production by encapsulated hMSCs. Encapsulated hMSC-treated hearts retained stem cells longer, showed improved revascularization, reduced scar formation, and resulted in improvement in left ventricular function as measured by transthoracic echocardiography (TTE) and cardiac magnetic resonance imaging (CMR). Encapsulation is a highly translatable platform for sustained paracrine stem cell function and a potential avenue for optimization of regenerative therapies.

Methods

Cell Culture

Commercially available bone marrow derived hMSC (Lonza) were cultured under standard conditions in mesenchymal stem cell growth media (Lonza) and used up to passage 6. To confirm that hMSC conformed to the accepted standard definition, cells were differentiated into adipogenic, osteo-genic, and chondrogenic phenotype by culture in hMSC Adipogenic BulletKit, hMSC Osteogenic BulletKit or hMSC Chondro BulletKit supplemented with TGF-β (Lonza). Differ-entiation was confirmed by Oil Red O stain for lipids, Alizarian Red stain for calcium and collagen Type II (ABcam) for cartilage. Cells were also immunophenotyped with flow cytometry for expression of CD73, CD90, CD105 and exclusion of CD14, CD20, CD34, and CD45 with MSC phenotyping kit (Miltenyi Biotec).

Encapsulation

One million hMSC per animal were suspended in 100 μL of 1% ultrapure low viscosity sodium alginate LVG (Novamatrix), encapsulated using an electrostatic encapsulator (Nisco) with a 0.17 mm nozzle, 10 mL/h flow rate, and 7 kV voltage, and gelled in a solution of 50 mmol/L $BaCl_2$. Encapsulated hMSC were washed in 0.9% saline and stored in Dulbecco's phosphate-buffered saline at 2 to 4°C up to 24 hours prior to implantation. Encapsulated cell viability was measured using LIVE/DEAD Viability/Cytotoxicity Kit (Invitrogen). The relative number of calcein-AM stained live cells to ethidium homodimer stained dead cells was quantified by serial z-stacked imaged obtained by confocal microscopy at 23 μm intervals.

Gel Production and Delivery

Sterile 4-arm PEG-maleimide macromer (Laysan Bio) was dissolved in 8 mmol/L triethanolamine and combined with a dithiol protease–cleavable peptide cross-linker (GCRDVPMSM RGGDRCG). Hydrogel components were sterilized in ethanol with centrifugal evaporation or by filtration through 0.45 μm centrifugal filter (Milipore). To this gel mixture were added one of the following: 1×10^6 encapsulated hMSCs, 1×10^6 non-encapsulated hMSCs, empty capsules without cells or nothing depending on treatment group. Gel formation on the myocardium was visually confirmed.

Animal Model

Rats were housed in the Emory University animal facility with a 12-hour light-dark cycle and allowed water and food ad libitum. Male nude rats (Crl:NIH-Foxn1^{rnu}) 200 to 250 gm (Harlen) underwent permanent ligation of the left anterior descending artery by an experienced microsurgeon (MEB) after anesthesia with inhaled isoflurane (2% to 3%). Infarction was confirmed by visualization of blanched and akinetic myocardium. Immediately after ligation, animals were treated with one of the following: gel only (MI+Gel), gel with empty capsules (MI+Gel+Empty Caps), gel with 1×10^6 non-encapsulated hMSCs (MI+Gel+hMSC), gel with 1×10^6 encapsulated hMSCs (MI+Gel+encapsulated hMSC) or given no treatment (MI). The chest was carefully closed without disturbing the location of the gel.

Bioluminescence Imaging (BLI)

hMSCs were transduced with a lentivirus expressing firefly luciferase and blasticidin resistance under the control of the constitutively active cytomegalovirus and respiratory syncytial virus promoters, respectively (GenTarget). Seventy-two hours after transduction, cells were transferred into standard media containing 10 μg/mL blasticidin (Sigma). Luciferase expression was confirmed with antiluciferase antibody (ABcam, 1:400) and luminescence imaging. Some animals were treated with 1×10^6 of the luciferase expressing hMSC either by direct injection (MI+ Direct Inject) into the peri-infarct area, by gel or encapsulated in gel. Animals were injected intraperitoneally with luciferin (40 mg/kg, Promega) and immediately imaged using a Xenogen IVIS 200 (Caliper). Luminescence was quantified in the region of interest over the heart using Living Image v. 4.2 (Caliper) software.

Cardiac Function Assessment

Animals were anesthetized with 1% to 2% inhaled isofluorane and underwent TTE using a Vevo 770™Imaging System (Visualsonics). During TTE assessment, heart rates were maintained above 350 beats per minute and all scans were done in a blinded fashion. LV end diastolic diameter (LVEDD), LV end systolic diameter (LVESD), and LV fractional shortening (LVFS) were measured with VisualSonics V 1.3.8 software from 2D long-axis views taken through the infarcted area.

A subset of animals underwent CMR with cardiac gaiting and data analysis using Segment (Medvisio). Electrocardiographic (ECG) needle electrodes and CMR-compatible Small Animal Monitoring & Gating System (SA Instrument) were used for cardiac gating. The rats were positioned in a temperature-controlled, purpose built cradle with a surface coil directly over the heart. The coil assembly was positioned in the horizontal bore of a Varian Inova 4.7 T 200/33 Imaging and Spectroscopy system using VNMR 6.1 software and tuned to approximately 200 Mhz. The gradient echo cine sequence (10-frames per heartbeat) was triggered on the R wave of the ECG signal. Endocardial border was traced using automated edge detection with manual adjustment in all segments in end systole and end diastole. The end systolic volume (LVESV) and diastolic volume (LVEDV) were used to calculate ejection fraction (LVEF). The institutional Animal Care and Use Committee of Emory University approved all protocols and procedures.

Morphometric and Immunohistochemical Analysis

Animals from each group were sacrificed by carbon dioxide inhalation at either 7 or 28 days after infarction and treatment. Bromodeoxyuridine (BrdU, 300 mg/kg) was injected intraperitoneally each day for 3 days prior to sacrifice. Consecutive sections from each heart were obtained after fixation in formalin and embedment in paraffin. A subset of hearts were also fixed and processed in Immuno-Bed plastic resin (Polysciences), sectioned at 2 μm, and stained with hematoxylin and eosin by standard protocol. Five μm paraffin sections through the peri-infarct area from each heart were stained with Masson's Trichrome and digital images of the whole heart taken using a microscope-mounted digital camera. Infarct area (blue) and non-infarct area (red) were quantified using NIH ImageJ software with automated thresholding in red-blue-green segmented images.

Paraffin sections were deparaffinized and stained with the following antibodies: rabbit anti-von Willebrand factor (vWF, Millipore, 1:200) and mouse antibromodeoxyuridine (BRDU) (Dako, 1:50). Prior to BrdU staining, sections were incubated in 2N HCl for 30 minutes at 37°C then neutralized in 0.1 mol/L sodium borate. Prior to vWF staining sections underwent antigen retrieval by heat in a pressure cooker at 100°C for 10 minutes in citrate buffer. Secondary biotinylated

antibody (Vector Labs, 1:400) then quantum dot 655 streptavidin-conjugate (Invitrogen, 1:200) was used to visualize antibody location. Apoptosis was quantified using In Situ Cell Death Detection Kit (Roche). Six peri-infarct image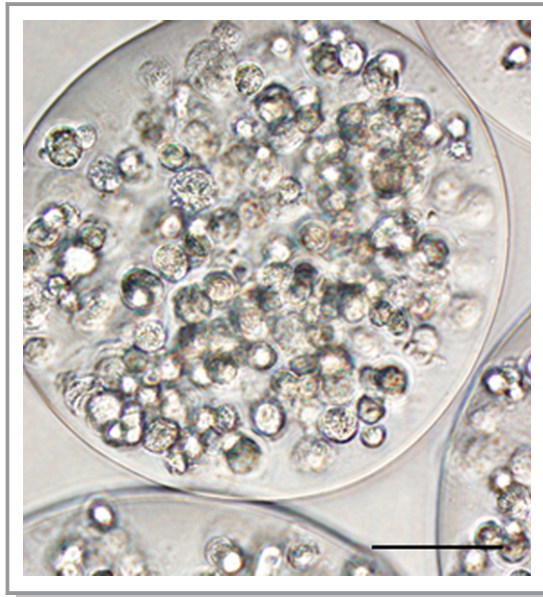s were taken from each section using Zeiss Axioskop at ×200 magnification. Fluorescence was quantified using Image Pro Plus.

Statistical Analysis

Statistical analysis was performed using Dunnett's test to compare variables in encapsulated hMSCs-treated animals to multiple controls and to weighted average of all control groups using the statistical software SPSS (IBM). BLI was analyzed using multi-dimensional analysis. Analysis of variance (ANOVA) was used when stated and data passed the D'Agostino & Pearson omnibus normality test ($P=0.6528$).

Results

Encapsulation and Microscopic Appearance of hMSC

Capsules were approximately 250 μm in diameter and each capsule contained between 200 and 250 cells (Figure 1). Prior to encapsulation, hMSCs were confirmed to be multipotent and expressed typical MSC markers (Figure 2). hMSC viability at the time of implantation was 95% after encapsulation, washing, and storage (Figure 3). Gels recovered 7 days after implantation were still adherent to the myocardium and contained capsules, blood vessels, and inflammatory cells. Gels were detectable up to 2 weeks after implantation but fully degraded by 28 days.

Figure 1. Histological appearance of encapsulated human mesenchymal stem cells (hMSCs). Light microscopic appearance of encapsulated hMSCs at the time of implantation with approximately 200 cells within each 250 μm capsule. (Scale bar=100 μm)
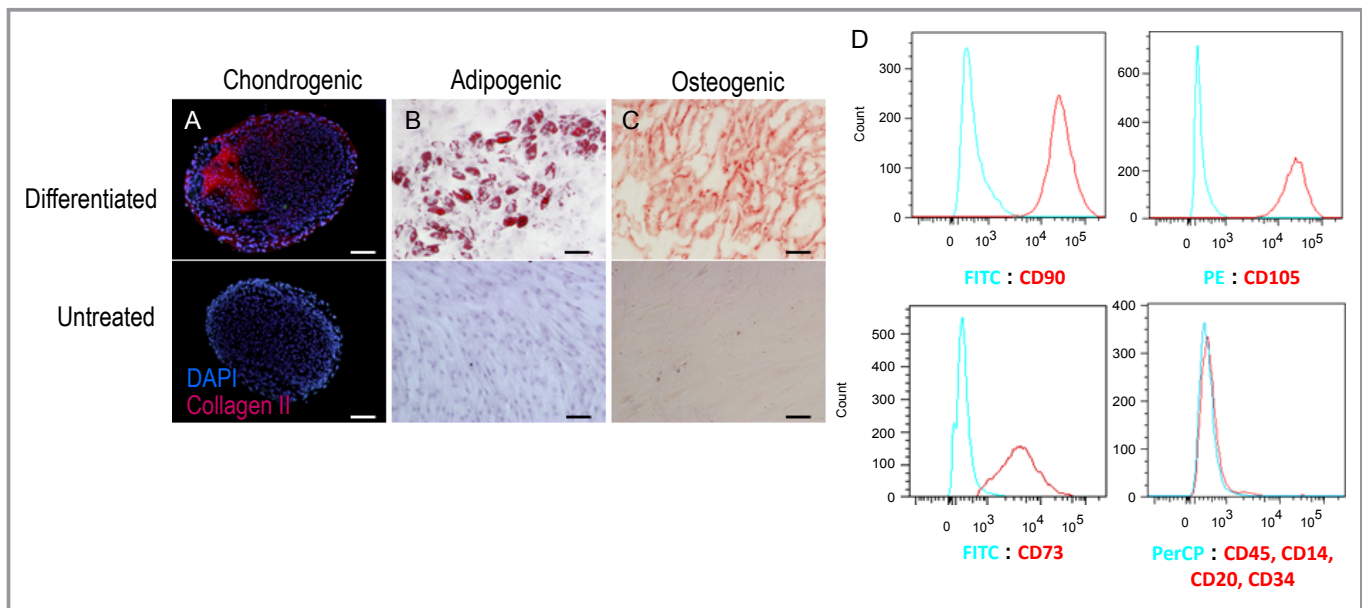
Figure 2. Multipotentcy of human mesenchymal stem cells (hMSCs). Prior to encapsulation, cultured hMSCs were differentiated into chondrogenic (A), adipogenic (B) and osteogenic (C) phenotype as shown by collagen type II, oil-red-O and Alizarin red staining, respectively. Control cells not treated with induction media remained un-differentiated. Fluorescence-activated cell sorting (FACS) analysis shows hMSCs express the typical MSC markers CD 73, CD 90, and CD 105 but not hematopoietic markers (D). Scale bar=100 μm.

Figure 3. Preserved cell viability after encapsulation and implantation. After encapsulation, storage, and implantation, viability of hMSCs was determined with a fluorescent viability assay which stained live cells green and dead cells red. Maximum intensity projection of capsule shows greater than 95% of cells were viable. Scale bar=100 μm. hMSCs indicates human mesenchymal stem cells.
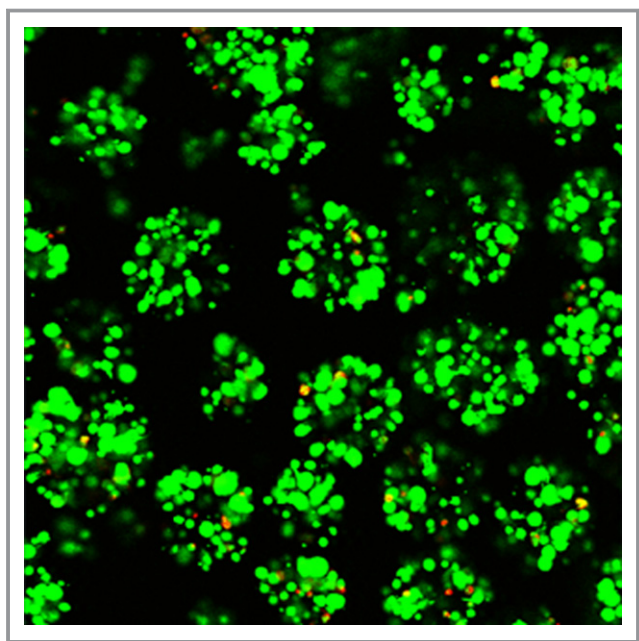
Encapsulated hMSCs Preserved Left Ventricular Function After MI

Two in vivo imaging modalities, TTE and CMR, were used to assess cardiac functional recovery post-MI. Both modalities showed similar and striking patterns of functional improvement in hearts treated with encapsulated hMSCs compared to all other control groups (Table; Figure 4). TTE showed reduction in LVESD ($P<0.01$) and increase in fractional shortening ($P<0.01$) at day 28 in animals treated with encapsulated hMSCs (Table). Functional improvement by fractional shortening by TTE was seen as early as 21 days (MI: 19±2%, n=9; MI+Gel: 30±3%, n=7; MI+Gel+hMSC: 19±2%, n=7; MI+Gel+Empty Caps: 23±2%, n=6; MI+Gel+encapsulated hMSC: 43±4%, n=8; $P<0.05$). Quantification of ventricular volumes by CMR at 28 days showed a marked improvement in ejection fraction (MI: 34±3%, MI+Gel: 35±3%, MI+Gel+hMSC: 39±2%, MI+Gel+ encapsulated hMSC: 56±1%; n=4 per group; $P<0.01$) and LVESV (MI: 304±13 μL, MI+Gel: 354±46 μL, MI+Gel+hMSC: 267±40 μL, MI+Gel+encapsulated hMSC: 160±11 μL; n=4 per group; $P<0.01$) in animals treated with encapsulated hMSCs compared to controls (Table; Figure 4). There was no difference in diastolic dimensions between the groups by either modality. In additional studies we compared delivery by encapsulation to the standard delivery technique of intramyocardial injection. Animals treated with cells delivered by intramyocardial injection showed worsened fractional shortening by TTE compared to encapsulated hMSC-treated animals at 28 days (MI+Direct Inject hMSC: 28±5%, n=7; MI+Gel+encapsulated hMSCs: 44±4%, n=8; $P<0.05$) (Figure 4D).

Retention of Transplanted hMSCs Near Infarcted Myocardium

Encapsulation and attachment of hMSCs to the heart by a hydrogel patch may inhibit several key mechanisms that limit stem cell retention in the myocardium, namely ejection from the myocardium by the force of contraction, washout by the myocardial capillaries and lymphatics, cell migration away from transplant site, and cell death. We transduced hMSCs with a lentiviral vector expressing firefly luciferase and

Table. Function Improvement in Cardiac Function as Seen by Transthoracic Echo (TTE) and Cardiac Magnetic Resonance Imaging (CMR)

	Echo, Day 28			CMR, Day 28		
	LVEDD, mm	LVESD, mm	FS, %	LVEDV, μL	LVESV, μL	EF, %
Sham	6.5±0.2	2.4±0.1	63±2	359±31	103±13	72±2
MI	7.0±0.5	5.4±0.5	22±3	464±31	304±13	34±3
MI + Gel	6.7±0.3	5.0±0.3	25±3	535±41	354±46	35±3
MI + Gel + Empty Cap	6.9±0.2	5.4±0.4	21±3	—	—	—
MI + Gel + hMSC	7.4±0.2	5.7±0.2	23±2	435±57	267±40	39±2
MI + Gel + encap hMSC	7.0±0.3	4.0±0.4*	44±4*	368±15	160±11*	56±1*

Animals treated with encapsulated human mesenchymal stem cells (hMSCs) had preserved end systolic diameter and fractional shortening by TTE. End diastolic diameter was unchanged. Similar results were found by MRI with decreased end systolic volume and improved EF in animals treated with encapsulated hMSCs at 28 days. EF indicates ejection fraction; FS, fractional shortening; LVEDD, left ventricular end diastolic dimension; LVEDV, left ventricular end diastolic volume; LVESD, left ventricular end systolic dimension; LVESV, left ventricular end systolic volume; MI, myocardial infarction.
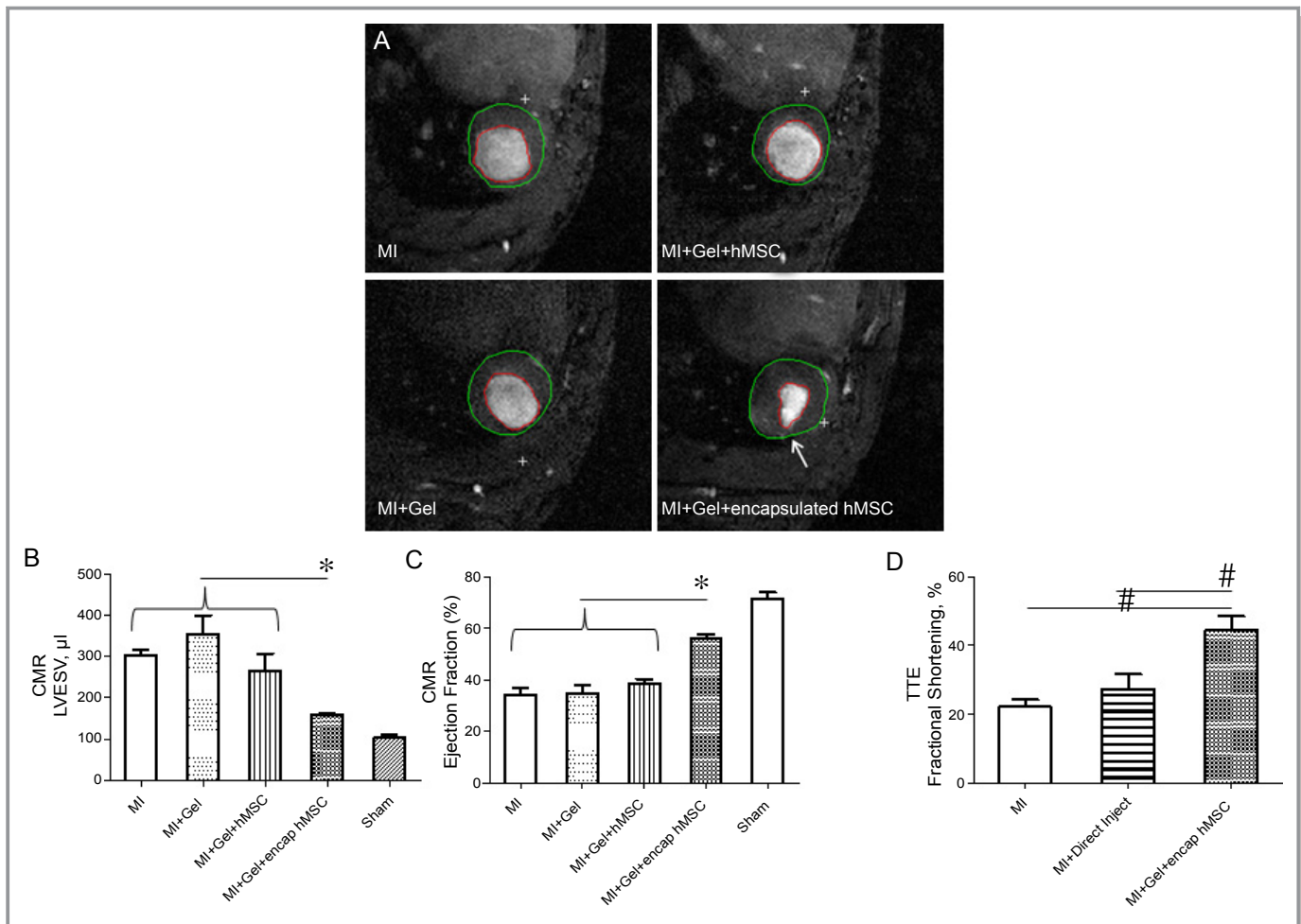*$P<0.05$ using Dunnett's test of multiple comparisons.

Figure 4. Detailed cardiac functional analysis by cardiac magnetic resonance imaging (CMR) and transthoracic echocardiography (TTE) showed improvement in animals treated with encapsulated human mesenchymal stem cells (hMSCs). A, Representative short axis CMR at end systole of animals treated with encapsulated hMSCs or controls. Myocardial thinning and chamber dilation, delineated by traced endocardium (red) and epicardium (green) was reduced in the encapsulated hMSC group (arrow). Quantification of end systolic volume (B) and ejection fraction (C) by CMR at day 28 showed improved contractile function in the encapsulated hMSC treated group (n=4 per group). D, TTE comparison of untreated animals (n=9) to animals treated with encapsulated hMSCs (n=7) or hMSCs delivered by direct injection (n=7) into the infarcted myocardium showed greater benefit of treatment with encapsulated cells. Data represent mean±SEM. *$P<0.05$ by Dunnett's test of multiple comparisons; #$P<0.05$ by analysis of variance (ANOVA). LVESV indicates left ventricular end systolic volume; MI, myocardial infarction.

measured BLI as an index of cell number. In vivo BLI showed greater retention of cells in animals treated with encapsulated hMSCs compared to delivery by direct injection at all time points (6 hours: $5\times10^6\pm1\times10^6$ versus $2\times10^6\pm6\times10^5$; day 1: $7\times10^6\pm2\times10^6$ versus $2\times10^6\pm7\times10^5$; day 3: $8\times10^6\pm3\times10^6$ versus $2\times10^6\pm8\times10^5$; day 5: $4\times10^6\pm7\times10^5$ versus $4\times10^5\pm3\times10^5$; day 7: $8\times10^5\pm2\times10^5$ versus $6\times10^4\pm9\times10^3$; $P<0.01$; n=8 per group; Figure 5). hMSCs were only visualized in noncardiac tissues in the direct injection group, suggesting that minimal washout or migration from the gel and capsules occurred (Figure 5A). The earliest feasible time point to image animals was approximately 6 hours after cell delivery. Quantification of BLI in the direct injection group showed a reduction in luminescence at this early time point despite

equal number of cells delivered ($P<0.05$). There was also an increase in signal in the encapsulated hMSC-treated animals which may have represented proliferation within the capsule. This peaked at day 3 then slowly declined (Figure 5B). By day 7, BLI was reduced in all animals and not detected in the direct injection animals (Figure 5). By 10 days the gel was largely dissolved and cell luminescence was not detectable over the heart.

Encapsulated hMSC Patch Minimized Scar Formation

We stained fixed sections of infarcted hearts with Masson's Trichrome to evaluate the extent of scar formation 28 days
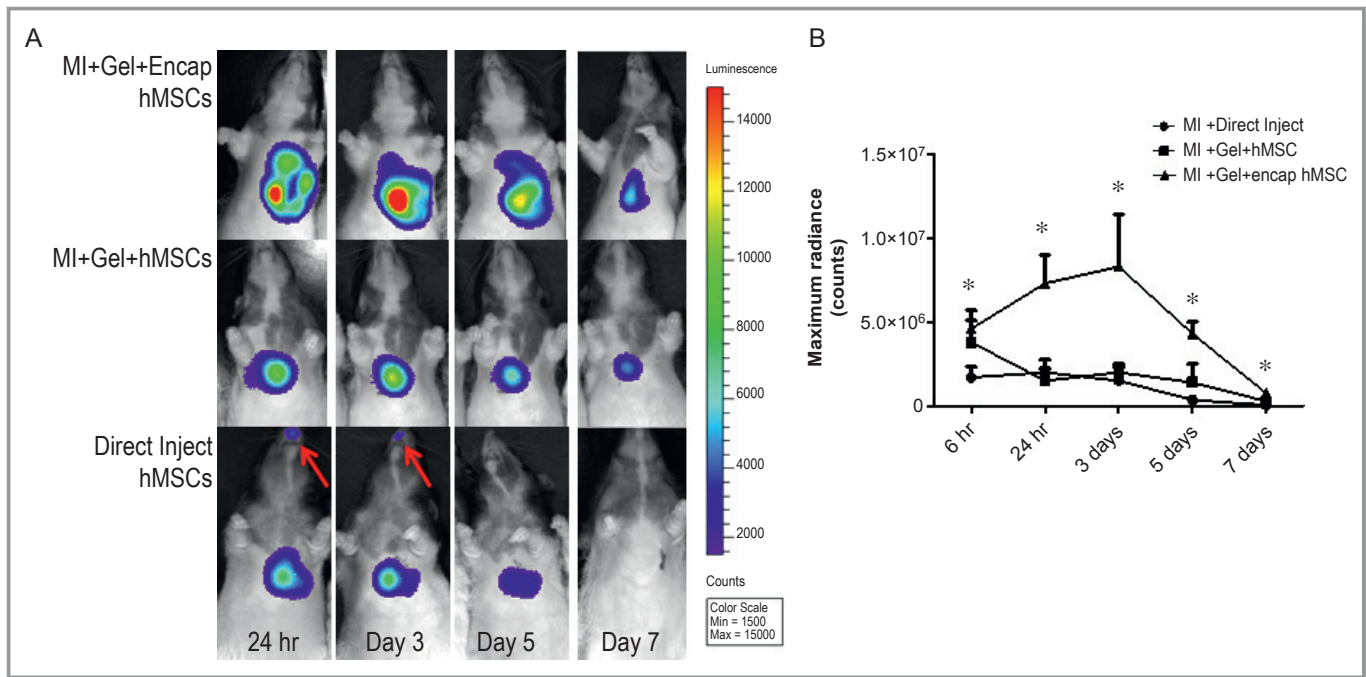
Figure 5. In vivo optical bioluminescence imaging (BLI) demonstrated increased retention and survival of encapsulated human mesenchymal stem cells (hMSCs). A, BLI image of representative animals from each group showed increased cell retention at all time points in the animal with encapsulated cells embedded in gel. Only animals in the direct injection group had detectable cells outside of the heart (arrow). B, Quantification of BLI signal in regions of interest over the heart showed greater signal in animals treated encapsulated hMSCs compared to direct injection at all time points (n=8 per group). Lower levels of signal at 6 hours in the direct injection group indicated rapid loss of cells in the first hours after implantation. Data represent mean±SEM. *$P<0.05$ by multidimensional analysis. MI indicates myocardial infarction.

after infarction and treatment. Quantification of the scar area showed that treatment with encapsulated hMSCs significantly reduced the scar area ($7\pm1\%$; n=6; $P<0.05$) compared to control hearts (MI: $12\pm1\%$, n=8; MI+Gel: $14\pm2\%$, n=7; MI+Gel+hMSC: $14\pm1\%$, n=7; MI+Gel+Empty Caps: $12\pm2\%$, n=5) (Figure 6).

Encapsulated hMSC Patch Promotes Increased Vascularity

We previously detected proangiogenic cytokines secreted by encapsulated hMSCs.[28] We quantified the degree of vascularization by staining sections of peri-infarct myocardium for the endothelial marker vWF and quantifying the number of microvessels in the peri-infarct area that were proliferating by BrdU staining. At 7 days, there was a large increase in proliferating endothelial cells in the peri-infarct area in animals treated with encapsulated hMSC (MI+Gel+encapsulated hMSCs: 127 ± 12 vessels/mm^2, n=8; MI: 78 ± 16 vessels/mm^2, n=8; MI+Gel: 33 ± 6 vessels/mm^2, n=8; MI+Gel+hMSC: 25 ± 5 vessels/mm^2, n=8; $P<0.001$). After 28 days, total microvessel density was significantly increased with encapsulated hMSCs (828 ± 56 vessels/mm^2; n=6; $P<0.01$) compared to other groups (MI: 121 ± 10 vessels/mm^2, n=7; MI+Gel: 153 ± 26 vessels/mm^2, n=5; MI+Gel+hMSC:

198 ± 18 vessels/mm^2, n=7; MI+Gel+Empty Caps: 215 ± 55 vessels/mm^2, n=5) and compared to normal muscle (231 ± 6 vessels/mm^2, n=3) (Figure 7).

Effects of Encapsulated hMSC Patch on Cardiomyocyte Proliferation and Apoptosis

There was no detectable difference in the rate of cardiomyocyte apoptosis by terminal deoxynucleotidyl transferase dUTP nick end labeling (TUNEL) staining at day 7 with each group having less than 0.25% apoptotic cells in the peri-infarct area (MI: $0.1\pm0.01\%$; MI+Gel: $0.1\pm0.03\%$; MI+Gel+hMSCs: $0.2\pm0.04\%$; MI+Gel+encapsulated hMSC: $0.2\pm0.10\%$; n=4 per group). To evaluate cardiomyocyte proliferation in the peri-infarct area, animals were administered BrdU to label the DNA of dividing cells. Quantification of BrdU-positive cardiomyocytes showed similar levels of proliferation among treatment groups (MI: $8\pm0.7\%$; MI+Gel: $3\pm0.6\%$; MI+Gel+hMSC: $5\pm0.9\%$, MI+Gel+encapsulated hMSCs: $9\pm0.7\%$; n=4 per group).

Discussion

Retention of viable cells at the site of delivery is a significant limitation of cell-based therapies for MI. In this study, we
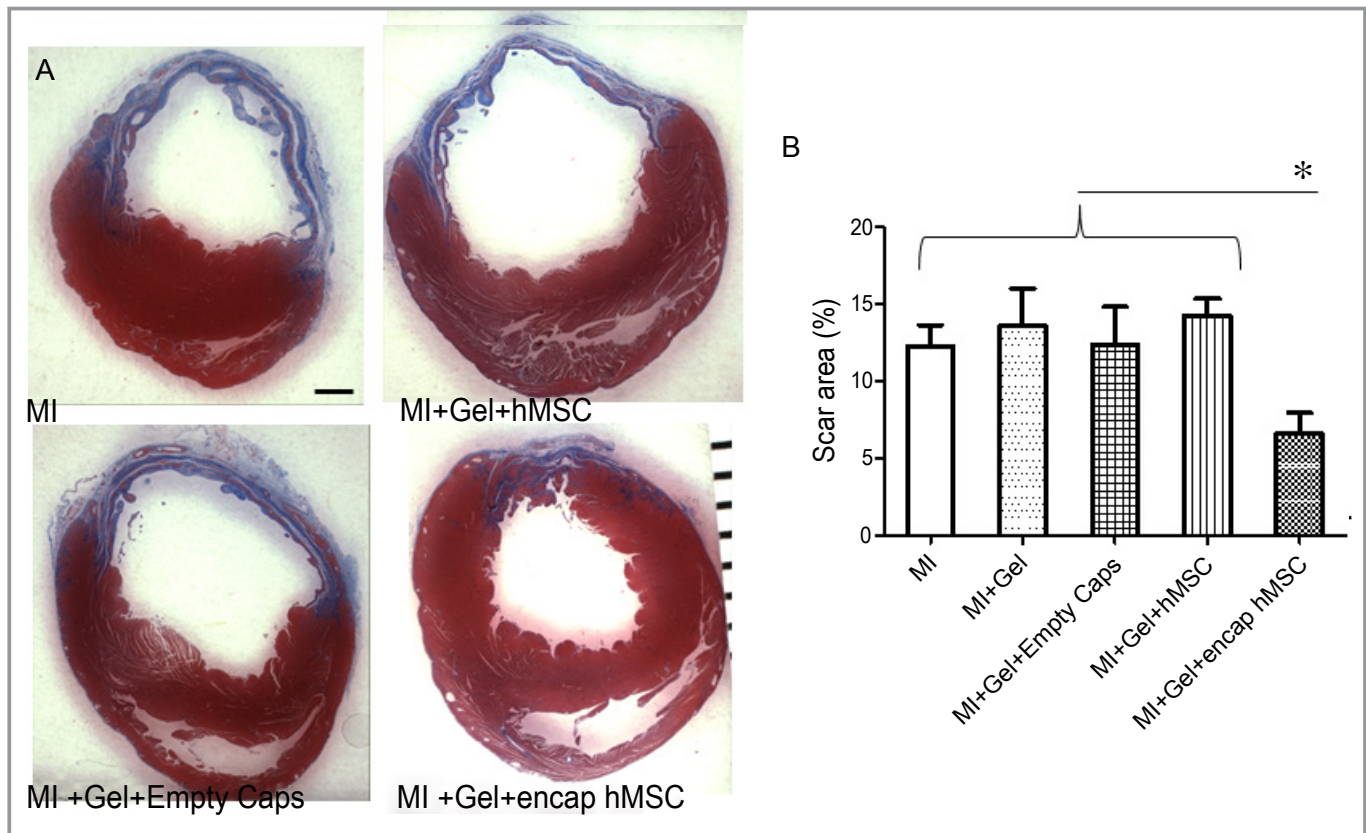
Figure 6. Treatment of hearts with encapsulated human mesenchymal stem cells (hMSC) post myocardial infarction reduced myocardial scarring at 28 days. A, Representative sections of infarcted hearts stained with Masson's Trichrome and treated with encapsulated hMSCs or control gels. Blue indicates fibrotic scar. ×15, scale bar=1 mm. B, Animals treated with encapsulated hMSCs showed reduced scar area (7±1%; n=6) at 28 days compared to control treated hearts (MI: 12±1%, n=8; MI+Gel: 14±2%, n=7; MI+Gel+hMSC: 14±1%, n=7; MI+Gel+Empty Caps: 12±2%, n=5). Data represent mean±SEM. *P<0.05. MI indicates myocardial infarction.

encapsulated hMSCs and measured their ability to augment cardiac function in the post-MI heart by paracrine action. Recent evidence has accumulated suggesting that stem cells delivered to the heart by intracoronary, intramyocardial, and intravenous routes have limited retention. The cells can fail to engraft, get washed out by lymphatic or vascular channels, or be cleared by the immune system.[38] In most large animal and human studies retention at 1 hour is less than 10%.[12–18] Delivery of cells by encapsulation may augment cell retention in the heart at early time points as the capsules are too large to wash out by lymphatic or venous channels and the physical structure of the capsule may shield the cells from immunoglobulins and cellular components of the immune system.[28]

We demonstrated that encapsulated cells were retained longer over the myocardium as detected by BLI at all time points including the earliest time point of 6 hours after delivery. Hearts treated with encapsulated hMSCs showed reduced scarring post-MI as well as greatly augmented peri-infarct microvasculature. Cardiac function as measured by TTE and CMR showed significant improvement in encapsulated hMSC-treated hearts. These data support encapsulation

as a readily translatable strategy to improve viable cell retention and efficacy for cell-based therapies for cardiovascular disease.

Improved Cardiac Function in Encapsulated hMSC Treatment

Two imaging modalities, TTE and CMR detected similar improvements in cardiac function in encapsulated hMSC-treated hearts (Figure 4; Table). Both fractional shortening and ejection fraction, measured by TTE and CMR respectively, improved significantly over controls. End systolic diameter and volume were the parameters that demonstrated the most dramatic improvement in encapsulated hMSC-treated hearts (Figure 4; Table). There was more variability in LVEDD and volume in all groups and we were not able to detect improvement in hearts treated with encapsulated hMSCs (Table). The control hearts with MI often developed apical aneurysmal dilations with preservation of the more basal myocardial segments. The preservation of the basal dimension of the heart may have partially masked changes in
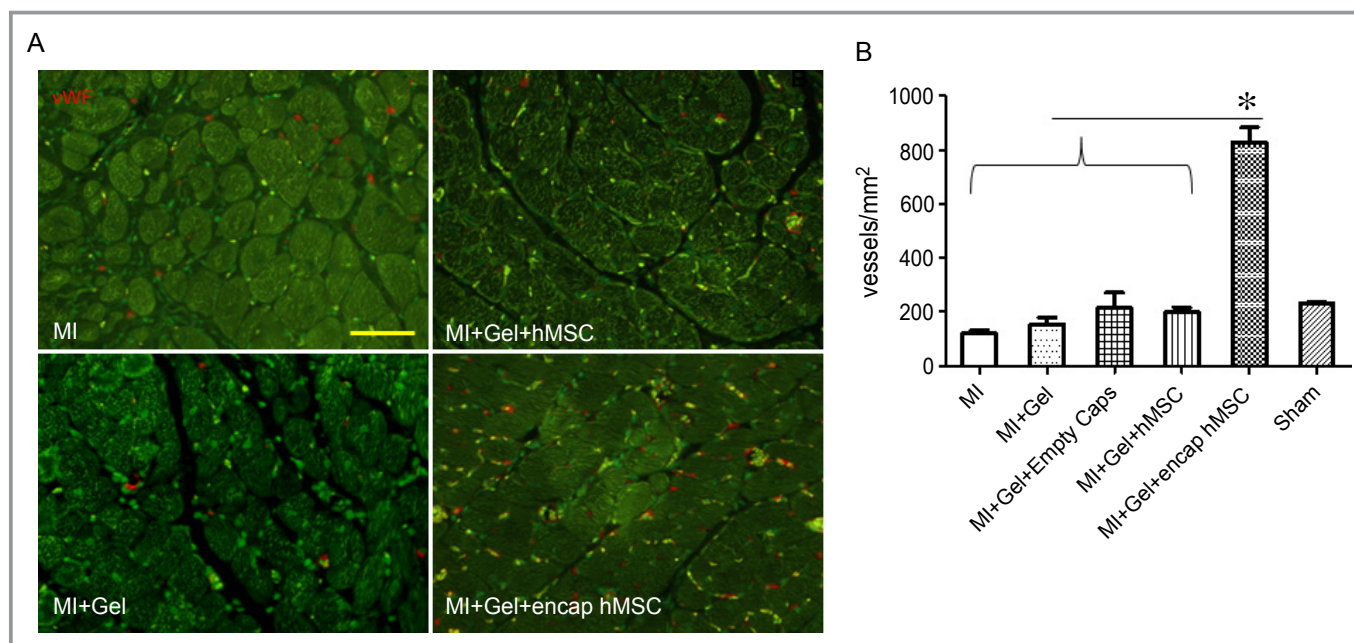
Figure 7. Microvascular density in peri-infarct myocardium was increased by treatment with encapsulated human mesenchymal stem cells (hMSCs). A, Representative sections from peri-infarct area of treatment groups showing von Willebrand factor stained capillaries (red) interspersed between auto-fluorescent cardiomyocytes (green). Scale bar=60 μm. B, Quantification of vessel density at day 28 showed a large increase in microvasculature in animals treated with encapsulated hMSCs (828 ± 56 vessels/mm^2; n=6; $P<0.01$) compared to other treatment groups (MI: 121 ± 10 vessels/mm^2, n=7; MI+Gel: 153 ± 26 vessels/mm^2, n=5; MI+Gel+hMSC: 198 ± 18 vessels/mm^2, n=7; MI+Gel+Empty Caps: 215 ± 55 vessels/mm^2, n=5), and normal muscle (231 ± 6 vessels/mm^2, n=3). Data represent mean$\pm$SEM. * $P<0.01$. MI indicates myocardial infarction.

volume of the apex as the entire ventricular volume was measured. Importantly, we did find a decrease in the size of the scar after MI by Masson's Trichrome staining in the animals treated with encapsulated cells embedded in gel (Figure 6). Encapsulated cell-treated animals likely had a more pronounced effect due to the prolonged cell retention over the myocardium compared to nonencapsulated or directly injected cells. Overall, the magnitude of the improvement seen in cardiac function in animals treated with encapsulated hMSC compared to nonencapsulated and directly injected cells illustrates the promise of this technique to optimize stem cell therapies for CVD.

Paracrine Action of Encapsulated hMSCs

We have designed our alginate capsules to optimize the paracrine action of transplanted cells. Previously published studies have used alginate to augment post-MI recovery in animal models, but have exploited different mechanisms of action. In one study, intramyocardially injected alginate served as a scaffold to both thicken and support the scar as well as a substrate for neovascularization.[39] This led to maintenance of scar thickness as well as functional improvement. We specifically designed and tested our capsules to not work as a structural support. Note that we detected no

functional or angiogenic benefit in the control groups treated with gel alone or gel with empty capsules. In another published strategy, alginate was seeded with myocyte precursors prior to implantation in the heart.[40] This study demonstrated electrical integration, as well as function improvement.[40] In contrast, we designed our capsules to optimize the paracrine function of the cells and prevented them from integrating into host tissue. This work represents the first cardiac application of alginate designed to encapsulate and optimize paracrine function of transplanted cells.

Proangiogenic Effects of Encapsulated hMSCs

In this study we detected a large increase in the peri-infarct microvasculature in hearts treated with encapsulated hMSCs. Control hearts had similar numbers of peri-infarct vessels when compared to sham treated hearts. Encapsulated cells could not directly incorporate into the tissue because they were retained inside the capsules and thus, their proangiogenic effect was likely paracrine. Revascularization is a critical step in myocardial preservation and regeneration and as a result, many candidate cells for regenerative therapy have been studied because of their ability to produce proangiogenic growth factors and cytokines. hMSCs are known to secrete a wide array of proangiogenic,[7] antiapoptotic,[5,6] and immune

modulatory[26] cytokines. hMSCs tend to respond to environmental cues such as hypoxia and modulate their secretome accordingly.[6,41] We have previously shown that encapsulated hMSCs produce proangiogenic cytokines such as angiogenin, angiopoietin 2, bFGF, hepatocyte growth factor, PlGF, and VEGF that diffuse out of the capsule.[28] Thus, the impact of preserved hMSC cell function on vascular growth is likely the mechanism through which there was preservation of myocardial function.

Potential for Translation of Encapsulation to Large Animal and Clinical Use

Encapsulation technology may be highly adaptable to larger animal models and translatable into human use. Highly pure alginate is already commercially available in GMP-grade purity. Clinical trials are currently underway using alginate in other applications including islet encapsulation for treatment of type I diabetes among others.[29,42] Encapsulation of hMSCs as described here could be scaled by at least an order of magnitude to accommodate large animal or human studies. In cardiac applications, encapsulated autologous hMSCs could be delivered as a patch (as in this study) or by intramyocardial injection.

Several limitations of this study will need investigation prior to translation of this technique. Animals used in this study were T cell deficient to prevent rejection of transplanted nonencapsulated cells. We have previously shown that our alginate capsules exclude IgG,[28] but the immune response to alginate or encapsulated cells may be more robust in immune competent animals. Alginate immunogenicity depends on composition, methodology of construction,[43] and to some extent may be species specific.[44] Therefore it will be important to track encapsulated cell viability and host response to alginate overtime in the immune competent patients. While our data suggest that the benefit of encapsulation is in large part due to prolonged presence of encapsulated cells in the heart and their paracrine release of proteins, many other mechanisms have been implicated. Exosome release,[45] micro RNA production,[46] and direct incorporation into developing tissues[47] have been shown to play a role in hMSC-mediated post-MI recovery. Thus, other mechanisms could contribute to the observed beneficial effects of cellular encapsulation.

In this study, we encapsulated hMSCs and attached them directly to the injured myocardium with a hydrogel patch. hMSCs were selected for this trial, but this technique could easily be applied to other cell types or genetically modified cells which may have some increased safety margin due to their containment within capsules. Encapsulation improved cell retention and minimized scar formation. As we move forward with evolving regenerative strategies, it will be critical to optimize not only the cell type, but also the delivery techniques to optimize the benefits of cell based therapies in humans.

Acknowledgments

Sources of Funding

Disclosures

None.

References

1. Asahara T, Murohara T, Alison S, Silver M, Zee RvD, Li T, Witzenbichler B, Schatteman G, Isner JM. Isolation of putative progenitor endothelial cells for angiogenesis. *Science*. 1997;275:964–967.

2. Yeh ETH, Zhang S, Wu HD, Körbling M, Willerson JT, Estrov Z. Transdifferentiation of human peripheral blood CD34+-enriched cell population into cardiomyocytes, endothelial cells, and smooth muscle cells in vivo. *Circulation*. 2003;108:2070–2073.

3. Kinnaird T, Stabile E, Burnett MS, Shou M, Lee CW, Barr S, Fuchs S, Epstein SE. Local delivery of marrow-derived stromal cells augments collateral perfusion through paracrine mechanisms. *Circulation*. 2004;109:1543–1549.

4. Gnecchi M, He H, Liang OD, Melo LG, Morello F, Mu H, Noiseux N, Zhang L, Pratt RE, Ingwall JS, Dzau VJ. Paracrine action accounts for marked protection of ischemic heart by akt-modified mesenchymal stem cells. *Nat Med*. 2005;11:367–368.

5. Takahashi M, Li T-S, Suzuki R, Kobayashi T, Ito H, Ikeda Y, Matsuzaki M, Hamano K. Cytokines produced by bone marrow cells can contribute to functional improvement of the infarcted heart by protecting cardiomyocytes from ischemic injury. *Am J Physiol Heart Circ Physiol*. 2006;291:H886–H893.

6. Xu M, Uemura R, Dai Y, Wang Y, Pasha Z, Ashraf M. In vitro and in vivo effects of bone marrow stem cells on cardiac structure and function. *J Mol Cell Cardiol*. 2007;42:441–448.

7. Kinnaird T, Stabile E, Burnett MS, Lee CW, Barr S, Fuchs S, Epstein SE. Marrow-derived stromal cells express genes encoding a broad spectrum of arteriogenic cytokines and promote in vitro and in vivo arteriogenesis through paracrine mechanisms. *Circ Res*. 2004;94:678–685.

8. Rehman J, Traktuev D, Li J, Merfeld-Clauss S, Temm-Grove CJ, Bovenkerk JE, Pell CL, Johnstone BH, Considine RV, March KL. Secretion of angiogenic and antiapoptotic factors by human adipose stromal cells. *Circulation*. 2004;109:1292–1298.

9. Aggarwal S, Pittenger MF. Human mesenchymal stem cells modulate allogeneic immune cell responses. *Blood*. 2005;105:1815–1822.

10. Caplan AI, Dennis JE. Mesenchymal stem cells as trophic mediators. *J Cell Biochem*. 2006;98:1076–1084.

11. Berry MF, Engler AJ, Woo YJ, Pirolli TJ, Bish LT, Jayasankar V, Morine KJ, Gardner TJ, Discher DE, Sweeney HL. Mesenchymal stem cell injection after myocardial infarction improves myocardial compliance. *Am J Physiol Heart Circ Physiol*. 2006;290:H2196–H2203.

12. Kang WJ, Kang H-J, Kim H-S, Chung J-K, Lee MC, Lee DS. Tissue distribution of 18f-fdg-labeled peripheral hematopoietic stem cells after intracoronary administration in patients with myocardial infarction. *J Nucl Med*. 2006;47:1295–1301.

13. Blocklet D, Toungouz M, Berkenboom G, Lambermont M, Unger P, Preumont N, Stoupel E, Egrise D, Degaute J-P, Goldman M, Goldman S. Myocardial homing of nonmobilized peripheral-blood CD34+ cells after intracoronary injection. *Stem Cells*. 2006;24:333–336.

14. Schächinger V, Aicher A, Döbert N, Röver R, Diener J, Fichtlscherer S, Assmus B, Seeger FH, Menzel C, Brenner W, Dimmeler S, Zeiher AM. Pilot trial on

determinants of progenitor cell recruitment to the infarcted human myocardium. *Circulation*. 2008;118:1425–1432.

15. Goussetis E, Manginas A, Koutelou M, Peristeri I, Theodosaki M, Kollaros N, Leontiadis E, Theodorakos A, Paterakis G, Karatasakis G, Cokkinos DV, Graphakos S. Intracoronary infusion of CD133+ and CD133−CD34+ selected autologous bone marrow progenitor cells in patients with chronic ischemic cardiomyopathy: cell isolation, adherence to the infarcted area, and body distribution. *Stem Cells*. 2006;24:2279–2283.

16. Hofmann M, Wollert KC, Meyer GP, Menke A, Arseniev L, Hertenstein B, Ganser A, Knapp WH, Drexler H. Monitoring of bone marrow cell homing into the infarcted human myocardium. *Circulation*. 2005;111:2198–2202.

17. Hou D, Youssef EA-S, Brinton TJ, Zhang P, Rogers P, Price ET, Yeung AC, Johnstone BH, Yock PG, March KL. Radiolabeled cell distribution after intramyocardial, intracoronary, and interstitial retrograde coronary venous delivery. *Circulation*. 2005;112:I-150–I-156.

18. Tossios P, Krausgrill B, Schmidt M, Fischer T, Halbach M, Fries JWU, Fahnenstich S, Frommolt P, Heppelmann I, Schmidt A, Schomäcker K, Fischer JH, Bloch W, Mehlhorn U, Schwinger RHG, Müller-Ehmsen J. Role of balloon occlusion for mononuclear bone marrow cell deposition after intracoronary injection in pigs with reperfused myocardial infarction. *Eur Heart J*. 2008;29: 1911–1921.

19. Assis ACM, Carvalho JL, Jacoby BA, Ferreira RLB, Castanheira P, Diniz SOF, Cardoso VN, Goes AM, Ferreira AJ. Time-dependent migration of systemically delivered bone marrow mesenchymal stem cells to the infarcted heart. *Cell Transplant*. 2010;19:219–230.

20. Bartunek J, Sherman W, Vanderheyden M, Fernandez-Aviles F, Wijns W, Terzic A. Delivery of biologics in cardiovascular regenerative medicine. *Clin Pharmacol Ther*. 2009;85:548–552.

21. Schuleri KH, Amado LC, Boyle AJ, Centola M, Saliaris AP, Gutman MR, Hatzistergos KE, Oskouei BN, Zimmet JM, Young RG, Heldman AW, Lardo AC, Hare JM. Early improvement in cardiac tissue perfusion due to mesenchymal stem cells. *Am J Physiol Heart Circ Physiol*. 2008;294:H2002–H2011.

22. Krause U, Harter C, Seckinger A, Wolf D, Reinhard A, Bea F, Dengler T, Hardt S, Ho A, Katus HA, Kuecherer H, Hansen A. Intravenous delivery of autologous mesenchymal stem cells limits infarct size and improves left ventricular function in the infarcted porcine heart. *Stem Cells Dev*. 2007;16:31–38.

23. Williams AR, Trachtenberg B, Velazquez DL, McNiece I, Altman P, Rouy D, Mendizabal AM, Pattany PM, Lopera GA, Fishman J, Zambrano JP, Heldman AW, Hare JM. Intramyocardial stem cell injection in patients with ischemic cardiomyopathy: functional recovery and reverse remodeling. *Circ Res*. 2011;108:792–796.

24. Schächinger V, Erbs S, Elsässer A, Haberbosch W, Hambrecht R, Hölschermann H, Yu J, Corti R, Mathey DG, Hamm CW, Süselbeck T, Assmus B, Tonn T, Dimmeler S, Zeiher AM. Intracoronary bone marrow–derived progenitor cells in acute myocardial infarction. *N Engl J Med*. 2006;355:1210–1221.

25. Lim F, Sun AM. Microencapsulated islets as bioartificial endocrine pancreas. *Science*. 1980;210:908–910.

26. Goren A, Dahan N, Goren E, Baruch L, Machluf M. Encapsulated human mesenchymal stem cells: a unique hypoimmunogenic platform for long-term cellular therapy. *FASEB J*. 2010;24:22–31.

27. Yu J, Du KT, Fang Q, Gu Y, Mihardja SS, Sievers RE, Wu JC, Lee RJ. The use of human mesenchymal stem cells encapsulated in rgd modified alginate microspheres in the repair of myocardial infarction in the rat. *Biomaterials*. 2010;31:7012–7020.

28. Landázuri N, Levit RD, Joseph G, Ortega-Legaspi JM, Flores CA, Weiss D, Sambanis A, Weber CJ, Safley SA, Taylor WR. Alginate microencapsulation of human mesenchymal stem cells as a strategy to enhance paracrine-mediated vascular recovery after hindlimb ischaemia. *J Tissue Eng Regen Med*. 2012; Dec 21 [Epub ahead of print] doi: 10.1002/term.1680

29. Scharp D, Swanson C, Olack B, Latta P, Hegre O, Doherty E, Gentile F, Flavin K, Ansara M, Lacy P. Protection of encapsulated human islets implanted without immunosuppression in patients with type i or type ii diabetes and in nondiabetic control subjects. *Diabetes*. 1994;43:1167–1170.

30. Phelps EA, Enemchukwu NO, Fiore VF, Sy JC, Murthy N, Sulchek TA, Barker TH, Garc̆a AJ. Maleimide cross-linked bioactive peg hydrogel exhibits improved reaction kinetics and cross-linking for cell encapsulation and in situ delivery. *Adv Mater*. 2012;24:64–70.

31. Karoubi G, Ormiston ML, Stewart DJ, Courtman DW. Single-cell hydrogel encapsulation for enhanced survival of human marrow stromal cells. *Biomaterials*. 2009;30:5445–5455.

32. Chi N-H, Yang M-C, Chung T-W, Chen J-Y, Chou N-K, Wang S-S. Cardiac repair achieved by bone marrow mesenchymal stem cells/silk fibroin/hyaluronic acid patches in a rat of myocardial infarction model. *Biomaterials*. 2012;33: 5541–5551.

33. Phelps EA, Landázuri N, Thulé PM, Taylor WR, Garc̆a AJ. Bioartificial matrices for therapeutic vascularization. *Proc Natl Acad Sci*. 2010;107: 3323–3328.

34. Go AS, Mozaffarian D, Roger VL, Benjamin EJ, Berry JD, Borden WB, Bravata DM, Dai S, Ford ES, Fox CS, Franco S, Fullerton HJ, Gillespie C, Hailpern SM, Heit JA, Howard VJ, Huffman MD, Kissela BM, Kittner SJ, Lackland DT, Lichtman JH, Lisabeth LD, Magid D, Marcus GM, Marelli A, Matchar DB, McGuire DK, Mohler ER, Moy CS, Mussolino ME, Nichol G, Paynter NP, Schreiner PJ, Sorlie PD, Stein J, Turan TN, Virani SS, Wong ND, Woo D, Turner MB. Heart disease and stroke statistics − 2013 update: a report from the American Heart Association. *Circulation*. 2013;127:e6–e245.

35. Hare JM, Traverse JH, Henry TD, Dib N, Strumpf RK, Schulman SP, Gerstenblith G, DeMaria AN, Denktas AE, Gammon RS, Hermiller JB Jr, Reisman MA, Schaer GL, Sherman W. A randomized, double-blind, placebo-controlled, dose-escalation study of intravenous adult human mesenchymal stem cells (prochymal) after acute myocardial infarction. *J Am Coll Cardiol*. 2009;54: 2277–2286.

36. Dill T, Schächinger V, Rolf A, Möllmann S, Thiele H, Tillmanns H, Assmus B, Dimmeler S, Zeiher AM, Hamm C. Intracoronary administration of bone marrow-derived progenitor cells improves left ventricular function in patients at risk for adverse remodeling after acute st-segment elevation myocardial infarction: results of the reinfusion of enriched progenitor cells and infarct remodeling in acute myocardial infarction study (repair-ami) cardiac magnetic resonance imaging substudy. *Am Heart J*. 2009;157:541–547.

37. Traverse JH, Henry TD, Ellis SG, Pepine CJ, Willerson JT, Zhao DXM, Forder JR, Byrne BJ, Hatzopoulos AK, Penn MS, Perin EC, Baran KW, Chambers J, Lambert C, Raveendran G, Simon DI, Vaughan DE, Simpson LM, Gee AP, Taylor DA, Cogle CR, Thomas JD, Silva GV, Jorgenson BC, Olson RE, Bowman S, Francescon J, Geither C, Handberg E, Smith DX, Baraniuk S, Piller LB, Loghin C, Aguilar D, Richman S, Zierold C, Bettencourt J, Sayre SL, Vojvodic RW, Skarlatos SI, Gordon DJ, Ebert RF, Kwak M, Moyé LA, Simari RD. Effect of intracoronary delivery of autologous bone marrow mononuclear cells 2 to 3 weeks following acute myocardial infarction on left ventricular function. *JAMA*. 2011;306:2110–2119.

38. Toma C, Wagner WR, Bowry S, Schwartz A, Villanueva F. Fate of culture-expanded mesenchymal stem cells in the microvasculature. *Circ Res*. 2009; 104:398–402.

39. Landa N, Miller L, Feinberg MS, Holbova R, Shachar M, Freeman I, Cohen S, Leor J. Effect of injectable alginate implant on cardiac remodeling and function after recent and old infarcts in rat. *Circulation*. 2008;117:1388–1396.

40. Dvir T, Kedem A, Ruvinov E, Levy O, Freeman I, Landa N, Holbova R, Feinberg MS, Dror S, Etzion Y, Leor J, Cohen S. Prevascularization of cardiac patch on the omentum improves its therapeutic outcome. *Proc Natl Acad Sci*. 2009; 106:14990–14995.

41. Gnecchi M, He H, Noiseux N, Liang OD, Zhang L, Morello F, Mu H, Melo LG, Pratt RE, Ingwall JS, Dzau VJ. Evidence supporting paracrine hypothesis for akt-modified mesenchymal stem cell-mediated cardiac protection and functional improvement. *FASEB J*. 2006;20:661–669.

42. Lee RJ, Hinson A, Helgerson S, Bauernschmitt R, Sabbah HN. Polymer-based restoration of left ventricular mechanics. *Cell Transplant*. 2013;22: 529–533.

43. Tam SK, Bilodeau S, Dusseault J, Langlois G, Hallé JP, Yahia LH. Biocompatibility and physicochemical characteristics of alginate–polycation microcapsules. *Acta Biomater*. 2011;7:1683–1692.

44. Vaithilingam V, Kollarikova G, Qi M, Lacik I, Oberholzer J, Guillemin GJ, Tuch BE. Effect of prolonged gelling time on the intrinsic properties of barium alginate microcapsules and its biocompatibility. *J Microencapsul*. 2011;28: 499–507.

45. Lai RC, Chen TS, Lim SK. Mesenchymal stem cell exosome: a novel stem cell-based therapy for cardiovascular disease. *Regen Med*. 2011;6:481–492.

46. Wen Z, Zheng S, Zhou C, Yuan W, Wang J, Wang T. Bone marrow mesenchymal stem cells for post-myocardial infarction cardiac repair: micrornas as novel regulators. *J Cell Mol Med*. 2012;16:657–671.

47. Toma C, Pittenger MF, Cahill KS, Byrne BJ, Kessler PD. Human mesenchymal stem cells differentiate to a cardiomyocyte phenotype in the adult murine heart. *Circulation*. 2002;105:93–98.